Potassium-chloride promiscuous channels in mitochondrial membranes

K. Ondrias, L. Malekova and O. Krizanova

Institute of Molecular Physiology and Genetics, Centre of Excellence for Cardiovascular Research, Slovak Academy of Sciences, 833 34 Bratislava, Slovakia

Abstract. Mitochondrial membranes isolated from a rat heart muscle were incorporated into a bilayer lipid membrane (BLM) and channel currents were measured in 250/50 mmol/l KCl *cis*/*trans* solutions. The channel currents measured from –40 to +40 mV had various linear voltage-current relationships and K^+/Cl^- permeability ratios at distinct voltage ranges. The channels possessed K^+-Cl^- promiscuous property. Depending on voltage, membrane permeability suddenly switched from K^+ over Cl^- to Cl^- over K^+ and back. The channels had $Cl^-/K^+ > 1$ permeability at potentials around 0 mV and the permeability was switched to $K^+/Cl^- > 1$ at more negative and positive potentials. The chloride channel blocker, 5-nitro-2-(phenylpropylamino)-benzoate (NPPB, 5×10^{-5} mol/l), influenced properties of the promiscuous channels – it activated potassium conductance of the channels.

Key words: Mitochondrial membrane — Promiscuous channels — NPPB — Single channel properties — BLM

Abbreviations: BLM, bilayer lipid membrane; E_{rev}, reversal potential; I-V, current-voltage relationship; NPPB, 5-nitro-2-(phenylpropylamino)-benzoate; caP channel, cation-anion promiscuous channel; VDAC, voltage-dependent anion-selective channel.

Introduction

Mitochondria play significant role not only in routine energy metabolism, but also in apoptotic and necrotic cell death. Permeability properties of outer and inner mitochondrial membranes are involved in these processes. Permeabilization of the outer mitochondrial membrane and subsequent release of intermembrane space proteins are important features of both models of cell death (Liu et al. 1996; Danial and Korsmeyer 2004). About 10 to 15% of the nuclear genes of eukaryotic organisms encode mitochondrial proteins. These proteins are synthesized in the cytosol and imported into mitochondria. Translocases in the outer and inner membrane of mitochondria mediate the import and intramitochondrial sorting of these proteins, in which ATP and the membrane potential are used as energy sources (Neupert and Herrmann 2007). Mitochondrial membrane permeability for different ions plays a role in modulation of mitochondrial membrane potentials, which is involved in their physiological and pathological functions (Zamzami et al. 1995; Cook et al. 1999; Vergun and Reynolds 2004; Glab et al. 2006). However, permeability properties of mitochondrial membrane for proteins, metabolites and ions are not fully understood. Therefore the aim of our work was to study K^+/Cl^- permeability of mitochondrial membrane channels.

Correspondence to: Karol Ondrias, Institute of Molecular Physiology and Genetics, Slovak Academy of Sciences, Vlárska 5, 833 34 Bratislava, Slovakia
E-mail: karol.ondrias@savba.sk

Materials and Methods

Chemicals

Lipids were obtained from Avanti Polar Lipids (Alabaster, AL, USA). Protease inhibitors were from Roche Diagnostics GmbH (Mannheim, Germany). All other chemicals were purchased from Sigma-Aldrich (Germany).

Isolation of mitochondrial membrane vesicles

An isolation of mitochondria and purification of mitochondrial membrane vesicles from the frozen hearts of male Wistar rats were done essentially as described previously (Malekova et al. 2007). Percol-purified mitochondria were sonicated 8 × 15 s at 35 kHz on ice and then centrifuged at 10,000 × *g* for 10 min. The obtained supernatant was again centrifuged at 100,000 × *g* for 30 min. The final mitochondrial membrane vesicle pellet was resuspended in buffer, frozen in liquid N_2 and stored at –70°C in small aliquots until reconstitution into bilayer lipid membrane (BLM).

Purity of isolated mitochondria

The purity of the isolated mitochondria was tested as described previously (Malekova et al. 2007). Contamination of the isolated mitochondria by sarcolemma was in the range of 0.6–1.5% ($n = 2$), and the contamination by sarcoplasmic reticulum membranes was in the range of 1–2% ($n = 2$). Based on the Western blot analysis with appropriate antibodies, the isolated mitochondria were contaminated by lysosomes, not by Golgi or nuclear membranes. The Percoll-purified mitochondrial membrane vesicles were not contaminated by lysosomes and contained inner and outer mitochondrial membranes as revealed by positive signals of COX-IV and VDAC1 antibodies against subunit V of cytochrome oxidase and voltage-dependent anion-selective channel (VDAC), respectively (Malekova et al. 2007).

BLM measurements

BLM was formed across an aperture (diameter ~0.1 mm) separating the *cis* and *trans* chambers using a mixture of dioleoyl-glycero-phosphatidylcholine and dioleoyl-glycero-phosphoethanolamine at a molar ratio of 3 : 2 in n-decane (20 mg/ml), similarly as in our previous study (Malekova et al. 2007). The composition of the *cis* and *trans* solutions was the same (in mmol/l): 0.1 $CaCl_2$, 0.3 EGTA, 10/5 Hepes/Tris, pH 7.4, but *cis*/*trans* KCl gradient was 250/50 mmol/l. The free Ca^{2+} concentration was calculated by WinMaxc32 version 2.50 (http://www.stanford.edu/_cpatton/maxc.html) and it was ~40 nmol/l. Under this condition, at 0 mV, a positive current means overall membrane Cl^- current over K^+ current, and a negative current means overall membrane K^+ current over Cl^- current. Fusion of membrane vesicles and measurement of single channel currents were done as described in our previous study (Malekova et al. 2007). Ionic permeability Cl^-/K^+ ratios were conventionally defined from the measured and extrapolated reversal potentials (E_{rev}) according to the modified Goldman–Hodgkin–Katz equation (Hayman et al. 1993). For present study we used single channels having irregular stable and constant opening and closing currents amplitude measured in the range from –40 to +40 mV. Regular "classical" Cl^-, K^+ and Ca^{2+} single mitochondrial channels with constant opening and closing amplitude were described in our previous works (Bednarczyk et al. 2004; Kominkova et al. 2004; Koszela-Piotrowska et al. 2007; Malekova et al. 2007).

Results

Channel properties

After incorporation of mitochondrial vesicles into BLM, various channels were observed. Some of them had non-constant opening and closing currents amplitude at the same voltage and had different conductance at different voltages (Figs. 1–6). For example, after changing of voltage from 0 to +40 mV, the channel shown in Fig. 1 (trace A), had four Cl^- conductance states, which decreased suddenly in three steps in time. The changing of voltage from –8 to –6 mV activated switch of the channel K^+ permeability to Cl^- one (Fig. 1, trace B). An overall channel current at 0 mV switched from Cl^- current to K^+ current in time (Fig. 2A). In order to study this phenomenon in more details we measured channel current from –40 to +40 mV at 2 mV steps, and voltage was changed each 9 ± 1 s. The voltage was changed manually what took about 1 s. A channel current, which was present >90% for 9 ± 1 s time interval was evaluated. Voltage dependence of the channel current measured from –40 to +40 mV is shown in Fig. 2B. The current at voltage interval –40 to +6 mV and +26 to +40 mV had conductance 307 pS, E_{rev} +6 mV, and permeability ratio $K^+/Cl^- = 1.4$. However, at voltages from +6 to +24 mV, the channel conductance was 788 pS, E_{rev} –12 mV, and permeability ratio Cl^-/K^+ was 2.1. The result indicates that the channel cation (K^+) permeability

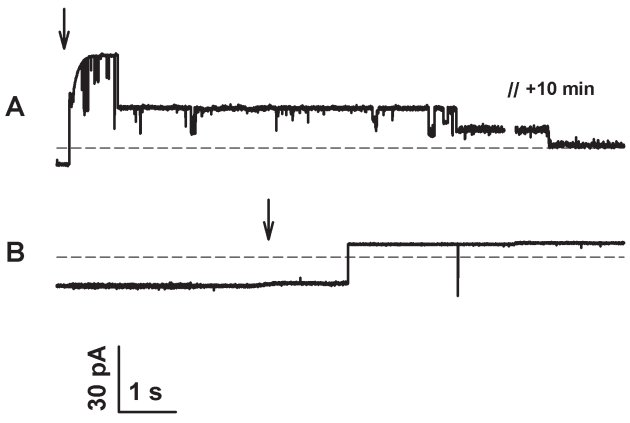

Figure 1. Single mitochondrial channel current. Arrows mark change of voltage from 0 to +40 mV (A) and from –8 to –6 mV (B). Dash lines mark 0 pA current.

was suddenly switched to the anion (Cl^-) one (Figs. 1, 2B). We called the channels (or channel complex), having such property, as cation-anion promiscuous (caP) channels. The promiscuity of the channel shown on Fig. 2B are clearly visible, but it was not clearly observed, when the voltage was changed from 0 mV to different voltages (Fig. 2A).

Some caP channels possessed more complicated voltage dependence of current-voltage relationship (I-V) (Figs. 3, 4). The channel shown in Fig. 3A had permeability ratio Cl^-/K^+ 2.5 and conductance 712 pS at the voltages from –8 to +16 mV, and it had permeability ratio K^+/Cl^- 4.9 and conductance 430 pS at the voltages from –40 to –38 mV, from –16 to +4 mV and from +16 to +40 mV. It possessed also permeability ratio K^+/Cl^- 1.8 and conductance 145 pS at the voltages from –32 to –22 mV. Reproducibility of single channel properties of most caP channels was poor. Even in a particular channel, it depended on a voltage and time history of the channel in BLM (Fig. 3B). I-V of the channel

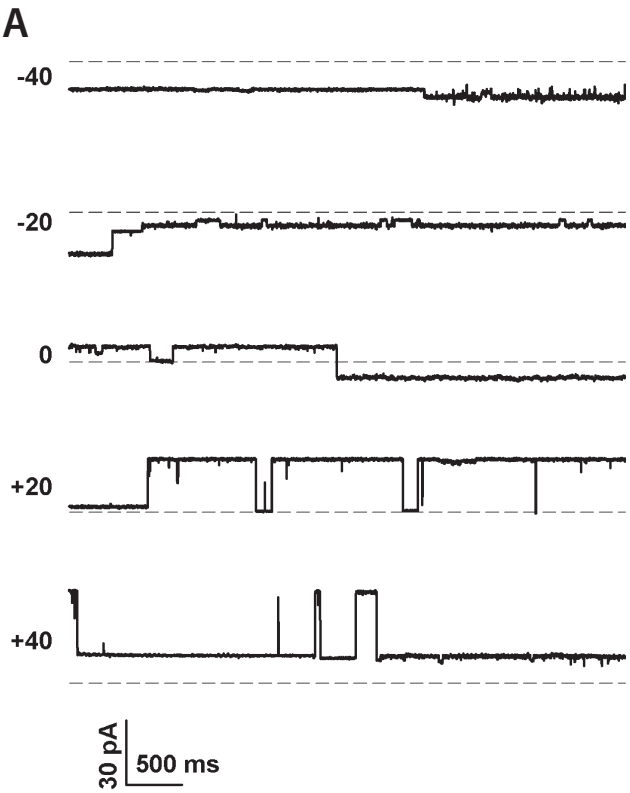

Figure 2. A. Single mitochondrial channel currents at different voltages. The *trans-cis* voltages (in mV) are depicted at left side of the traces. Dash lines mark 0 pA current. **B.** Voltage dependence (from –40 to +40 mV) of channel current. *Cis* and *trans* solutions contained 2 mmol/l $MgCl_2$, and *cis* solution contained also 100 μmol/l Ca^{2+} free. Dash lines indicate channel conductances.

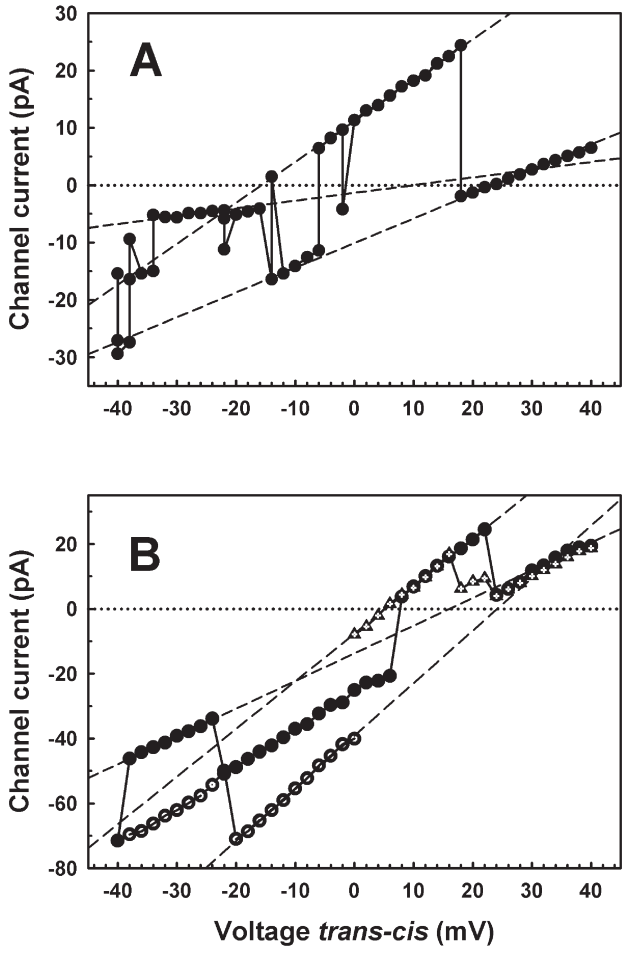

Figure 3. A. Voltage dependence (from –40 to +40 mV) of channel current. Dash lines indicate channel conductances. **B.** Voltage dependence of channel current. The voltage was applied from 0 to –40 mV (open circles), from –40 to +40 mV (full circles) and from –40 to 0 mV (open triangles). Dash lines indicate channel conductances.

shown in Fig. 3A was changed after 5 min incubation at 0 mV, when the Cl^- channel current at 0 mV switched from +5.8 to –8.4 pA K^+ one. The channel behavior depended also on applying voltage steps. The voltage switches of I-V were different when the applied voltage steps were in negative or positive values (Figs. 3B, 4A).

The channel conductance shown in Fig. 4A had four different I-V and four different K^+/Cl^- permeabilities in the range from –40 mV to +40 mV. Interestingly, there was positive correlation between the conductances and the K^+/Cl^- permeability ratios (Fig. 4B) derived from the Fig. 4A.

Effect of NPPB

We tested effect of 5-nitro-2-(phenylpropylamino)-benzoate (NPPB) on two relatively stable caP channels (Figs. 4, 5). NPPB (50 μmol/l) influenced conductivity and transition points of the channels. It decreased Cl^- current at high positive voltage (from +36 to +40 mV) and induced new conductance states of K^+ current at negative voltages (from +4 to –36 mV) (Fig. 4B). It induced switch from Cl^- to K^+ current at 0 mV and decreased Cl^- current at >+4 mV and <–16 mV (Fig. 5B). Fig. 6 shows examples of the activation effect of NPPB on three caP channels. NPPB activated K^+ current at 0 mV of the caP channels, which had different conductances.

Discussion

In the present study we repoted that mitochondrial membrane vesicles contained channels having voltage-dependent potassium-chloride permeability. Because of the voltage-dependent cation-anion channel permeability, we called them caP channels. So far only one study reported an ion promiscuous channel observed in plasma membrane of cardiac myocytes (Santana et al. 1998). The channel had Na^+-Ca^{2+} promiscuity, which was induced by an activation of a β-adrenergic receptor or protein kinase A, or by cardiotonic steroids such as ouabain and digoxin. To our knowledge, there was no caP channel reported so far.

Since observed caP channels had not regular single channel stable and constant opening and closing currents, at the same voltage, we may assume that they have different structure in comparison with "classical" membrane channels and they are formed by protein complex rather than by single protein. The caP channels had various single channel properties. It is not clear whether the properties result from different channels incorporated in BLM or from a variability of single channel properties of one particular type of channel. From the positive correlation between the conductances and the K^+/Cl^- permeability ratios (Fig. 4B) it is supposed that

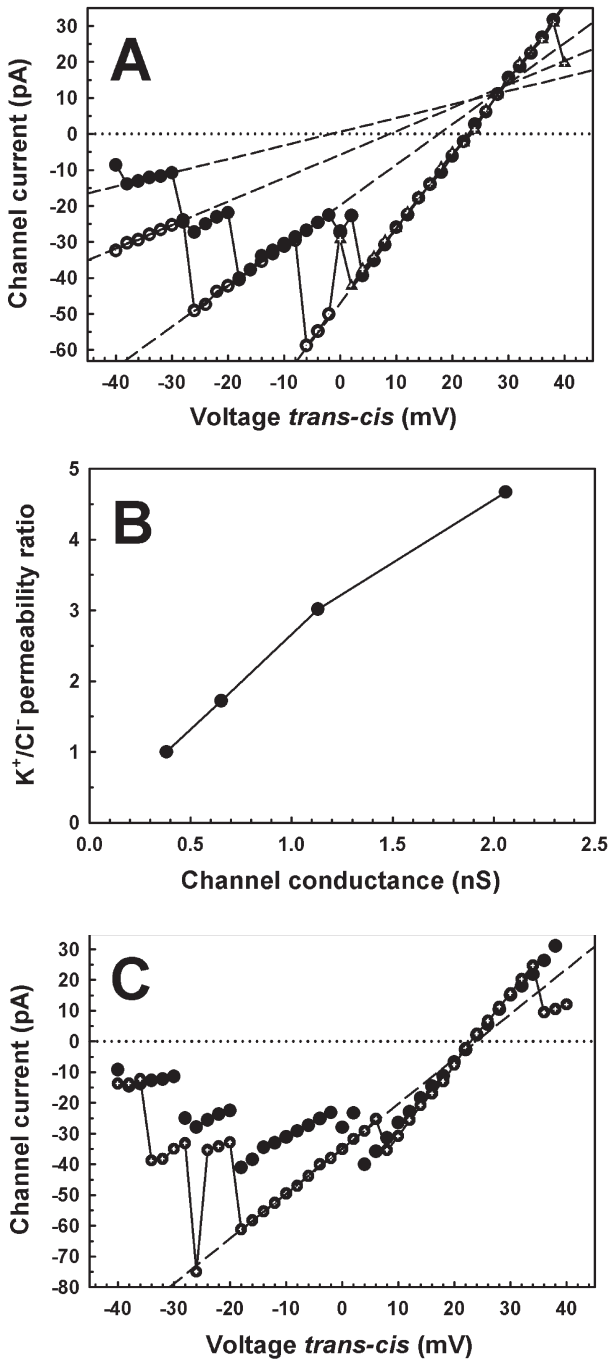

Figure 4. A. Voltage dependence of channel current. The voltage was applied from 0 to –40 mV (open circles), from –40 to +40 mV (full circles) and from –40 to 0 mV (open triangels). Dash lines indicate channel conductances. **B.** Relationship between the channel conductances and the K^+/Cl^- permeability ratios. **C.** Voltage dependence of control channel current (data from A, full circles) and the current in the presence of 50 μmol/l NPPB in *cis* and *trans* solutions (open circles). The voltage was applied from –40 to +40 mV. Dash line indicates channel conductance: the current at the voltages from –26 to +6 mV had conductance 1.46 nS and E_{rev} +23 mV and permeability ratio $K^+/Cl^- = 4.5$.

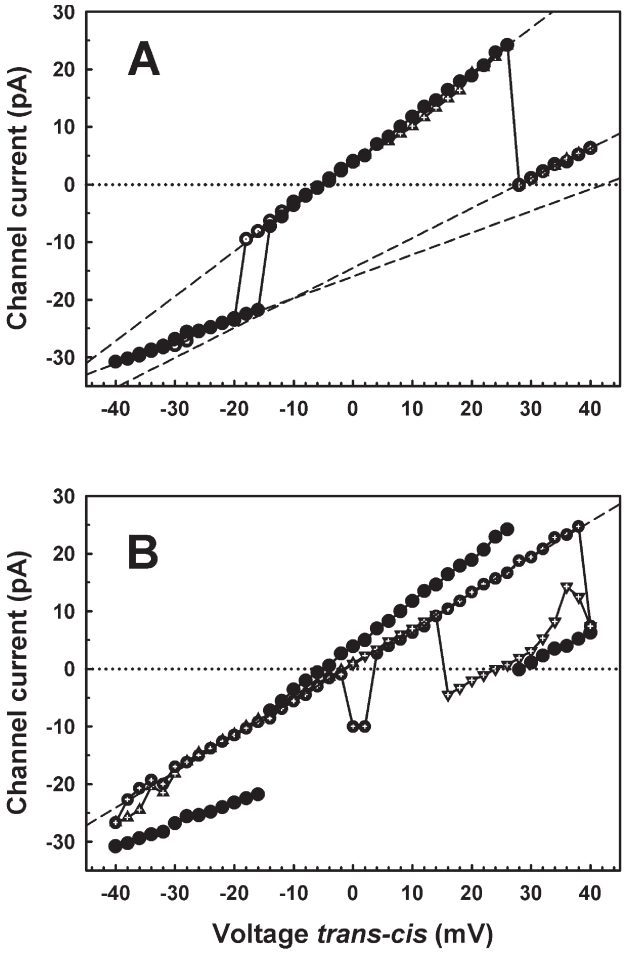

Figure 5. A. Voltage dependence of channel current. The voltage was applied from 0 to –40 mV (open circles), from –40 to +40 mV (full circles) and from –40 to 0 mV (open triangles). Dash lines indicate channel conductances. The current at the voltages from –40 to –18 mV had conductance 379 pS, E_{rev} +42 mV, and permeability ratio K^+/Cl^- = 119. At the voltages from –18 to +26 mV, the channel conductance was 776 pS, E_{rev} = –6 mV, and permeability ratio was Cl^-/K^+ = 1.4. At the voltages from +26 to +40 mV conductance 520 pS, E_{rev} +27 mV, and permeability ratio K^+/Cl^- = 6.4. **B.** Voltage dependence of control channel current (data from A, full circles) and the current in the presence of 50 μmol/l NPPB in *cis* and *trans* solutions (open symbols). The voltage in the presence of NPPB was applied from 0 to –40 mV (open triangles up), from –40 to +40 mV (open circles) and from +40 to 0 mV (open triangles down). Dash line indicates channel conductance: the current at the voltages from –38 to +40 mV had conductance 620 pS and E_{rev} –2 mV and permeability ratio Cl^-/K^+ = 1.1.

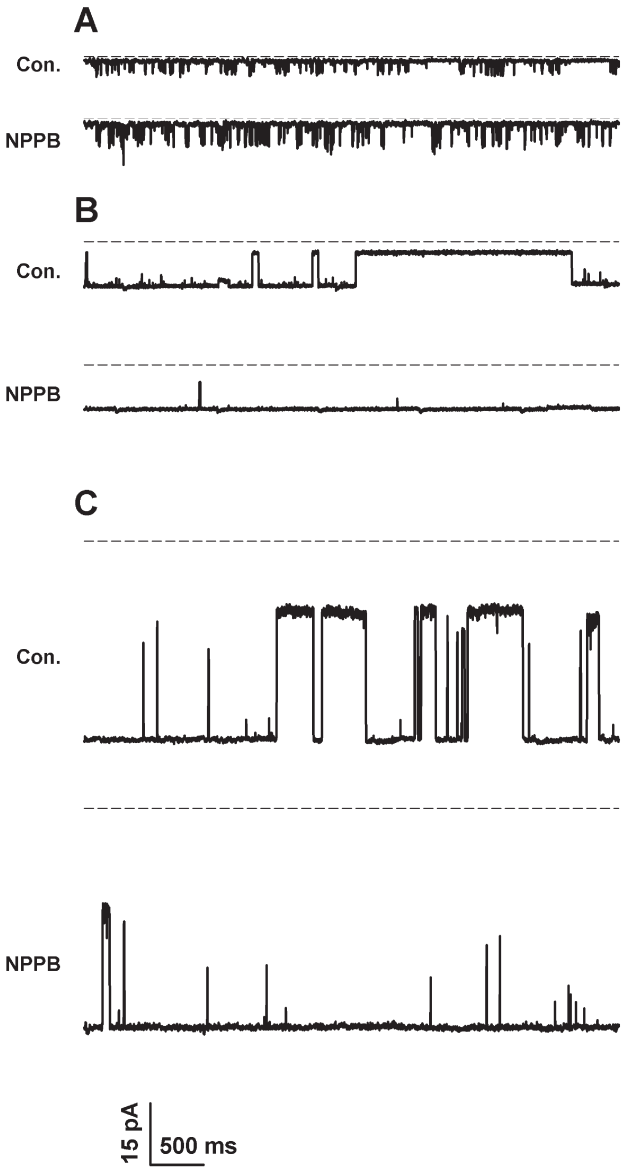

Figure 6. Effect of 50 μmol/l 5-nitro-2-(phenylpropylamino)-benzoate (NPPB) (A and B – NPPB in *cis*, C – NPPB in *cis* and *trans*) on single mitochondrial channel currents at 0 mV in three experiments. Dash lines mark 0 pA current. Down deflections indicate K^+ current. Con., control.

the increase in conductance is not a result of an increased channel pore diameter.

The origin of the caP channels is unclear, since our isolated vesicles contained both outer and inner mitochondrial membranes, which contain a wide variety of selective transport pathways for ions, metabolites and proteins. Many of them has channel-like properties, for example VDAC, translocase of the outer mitochondrial membrane, adenine nucleotide translocase, mitochondrial permeability transition pore, mitochondrial apoptosis-induced channel, sphingosine and ceramide channels (Colombini 1989; Ruck et al. 1998; O'Rourke 2000; Becker et al. 2005; Siskind et al. 2005; Bathori et al. 2006; Dejean et al. 2006; Glab et al. 2006; Belizario et al. 2007). A molecular structure and/or

components of most of the channel-like structures are variable or remain to be determined. Inner mitochondrial membrane potential and its fluctuation play a role in many physiological and pathological processes. Membrane potential of outer mitochondrial membrane was supposed from measurement of pH gradient across the membrane (Porcelli 2005). We may assume that the caP channels could be a part of the mitochondrial membrane structures involved in membrane passive or selective transport sensitive to voltage.

Properties of the caP channels have some similarities with VDAC, which was reported to show a high and symmetrical voltage-dependent conductance, which was highest at low potentials around 0 mV and decreased at higher positive or negative potentials (>30–60 mV) (Colombini 1989; Shoshan-Barmatz et al. 2006). However, it was also reported that at low free Ca^{2+} concentration (600 nmol/l), VDAC conductance decreased significiantly (Bathori et al. 2006) what was not observed in our experiments using free Ca^{2+} concentration ~40 nmol/l.

We tested whether caP channels are sensitive to NPPB, which was reported to inhibit a chloride uptake into mitochondria (Arnould et al. 2003), uncoupled mitochondria (Lukacs et al. 1991) and prevented apoptosis in mouse cardiomyocytes (Wang et al. 2005; Malekova et al. 2007). NPPB influenced properties of caP channels what may indicate that NPPB-caP channel interaction may be responsible for some of its numerous biological effects.

Acknowledgments. The study was supported by grants: APVV 0397-07 and VEGA 2/6012/6.

References

Arnould T., Mercy L., Houbion A., Vankoningsloo S., Renard P., Pascal T., Ninane N., Demazy C., Raes M. (2003): mtCLIC is up-regulated and maintains a mitochondrial membrane potential in tDNA-depleted L929 cells. FASEB J. **17**, 2145–2147

Bathori G., Csordas G., Garcia-Perez C., Davies E., Hajnoczky G. (2006): Ca^{2+}-dependent control of the permeability properties of the mitochondrial outer membrane and voltage-dependent anion-selective channel (VDAC). J. Biol. Chem. **281**, 17347–17358

Becker L., Bannwarth M., Meisinger C., Hill K., Model K., Krimmer T., Casadio R., Truscott K. N., Schulz G. E., Pfanner N., Wagner R. (2005): Preprotein translocase of the outer mitochondrial membrane: reconstituted Tom40 forms a characteristic TOM pore. J. Mol. Biol. **353**, 1011–1020

Bednarczyk P., Kicinska A., Kominkova V., Ondrias K., Dolowy K., Szewczyk A. (2004): Quinine inhibits mitochondrial ATP-regulated potassium channel from bovine heart. J. Membr. Biol. **199**, 63–72

Belizario J. E., Alves J., Occhiucci J. M., Garay-Malpartida M., Sesso A. (2007): A mechanistic view of mitochondrial death decision pores. Braz. J. Med. Biol. Res. **40**, 1011–1024

Colombini M. (1989): Voltage gating in the mitochondrial channel, VDAC. J. Membr. Biol. **111**, 103–111

Cook S. A., Sugden P. H., Clerk A. (1999): Regulation of Bcl-2 family proteins during development and in response to oxidative stress in cardiac myocytes association with changes in mitochondrial membrane potential. Circ. Res. **85**, 940–949

Danial N. N., Korsmeyer S. J. (2004): Cell death: critical control points. Cell **116**, 205–219

Dejean L. M., Martinez-Caballero S., Kinnally K. W. (2006): Is MAC the knife that cuts cytochrome c from mitochondria during apoptosis? Cell Death Differ. **13**, 1387–1395

Glab M., Lojek A., Wrzosek A., Dolowy K., Szewczyk A. (2006): Endothelial mitochondria as a possible target for potassium channel modulators. Pharmacol. Rep. **58**, 89–95

Hayman K. A., Spurway T. D., Ashley R. H. (1993): Single anion channels reconstituted from cardiac mitoplasts. J. Membr. Biol. **136**, 181–190

Kominkova V., Novotova M., Ondrias K., Ravingerova T., Szewczyk A. (2004): Mitochondrial channels permeable by calcium ions. Toxicol. Mech. Methods **14**, 35–39

Koszela-Piotrowska I., Choma K., Bednarczyk P., Dolowy K., Szewczyk A., Kunz W. S., Malekova L., Kominkova V., Ondrias K. (2007): Stilbene derivatives inhibit the activity of the inner mitochondrial membrane chloride channels. Cell. Mol. Biol. Lett. **12**, 493–508

Liu X., Kim C. N., Yang J., Jemmerson R., Wang X. (1996): Induction of apoptotic program in cell-free extracts: requirement for dATP and cytochrome c. Cell **86**, 147–157

Lukacs G. L., Nanda A., Rotstein O. D., Grinstein S. (1991): The chloride channel blocker 5-nitro-2-(3-phenylpropylamino) benzoic acid (NPPB) uncouples mitochondria and increases the proton permeability of the plasma membrane in phagocytic cells. FEBS Lett. **288**, 17–20

Malekova L., Tomaskova J., Novakova M., Stefanik P.,Kopacek J., Lakatos B., Pastorekova S., Krizanova O., Breier A., Ondrias K. (2007): Inhibitory effect of DIDS, NPPB, and phloretin on intracellular chloride channels. Pflügers Arch. **455**, 349–357

Neupert W., Herrmann J. M. (2007): Tanslocation of proteins into mitochondria. Annu. Rev. Biochem. **76**, 723–749

O'Rourke B. (2000): Pathophysiological and protective roles of mitochondrial ion channels. J. Physiol. **529,** 23–36

Porcelli A. M., Ghelli A., Zanna C., Pinton P., Rizzuto R., Rugolo M. (2005): pH difference across the outer mitochondrial membrane measured with a green fluorescent protein mutant. Biochem. Biophys. Res. Commun. **326**, 799–804

Ruck A., Dolder M., Wallimann T., Brdiczka D. (1998): Reconstituted adenine nucleotide translocase forms a channel for small molecules comparable to the mitochondrial permeability transition pore. FEBS Lett. **426**, 97–101

Santana L. F., Gomez A. M., Lederer W. J. (1998): Ca^{2+} flux through promiscuous cardiac Na^{+} channels: slip-mode conductance. Science **279**, 1027–1033

Shoshan-Barmatz V., Israelson A., Brdiczka D., Sheu S. S. (2006): The voltage-dependent anion channel (VDAC): function in intracellular signalling, cell life and cell death. Curr. Pharm. Des. **12**, 2249–2270

Siskind L. J., Fluss S., Bui M., Colombini M. (2005): Sphingosine forms channels in membranes that differ greatly from those formed by ceramide. J. Bioenerg. Biomembr. **37**, 227–236

Vergun O., Reynolds I. J. (2004): Fluctuations in mitochondrial membrane potential in single isolated brain mitochondria: modulation by adenine nucleotides and Ca^{2+}. Biophys. J. **87**, 3585–3593

Wang X., Takahashi N., Uramoto H., Okada Y. (2005): Chloride channel inhibition prevents ROS-dependent apoptosis induced by ischemia-reperfusion in mouse cardiomyocytes. Cell. Physiol. Biochem. **16**, 147–154

Zamzami N., Marchetti P., Castedo M., Zanin C., Vayssiere J. L., Petit P. X., Kroemer G. (1995): Reduction in mitochondrial potential constitutes an early irreversible step of programmed lymphocyte death *in vivo*. J. Exp. Med. **181**, 1661–1672

Final version accepted: February 14, 2008

Effects of voltage sensitive dye di-4-ANEPPS on guinea pig and rabbit myocardium

M. Novakova[1], J. Bardonova[2], I. Provaznik[2], E. Taborska[3], H. Bochorakova[3], H. Paulova[3] and D. Horky[4]

[1] *Department of Physiology, Faculty of Medicine, Masaryk University, Brno, Czech Republic*
[2] *Department of Biomedical Engineering, Faculty of Electrical Engineering and Communication, University of Technology, Brno, Czech Republic*
[3] *Department of Biochemistry, Faculty of Medicine, Masaryk University, Brno, Czech Republic*
[4] *Department of Histology and Embryology, Faculty of Medicine, Masaryk University, Brno, Czech Republic*

Abstract. Voltage-sensitive dyes (VSDs) are used to record transient potential changes in various cardiac preparations. In our laboratory, action potentials have been recorded by optical probe using di-4-ANEPPS. In this study, the effects of two different ways of staining were compared in guinea pig and rabbit isolated hearts perfused according to Langendorff: staining either by coronary perfusion with low dye concentration or with concentrated dye as a bolus into the aorta. Staining with low dye concentration lead to its better persistence in the tissue. Electrogram and coronary flow were monitored continuously. During the staining and washout of the dye, prominent electrophysiological changes occurred such as a decrease in spontaneous heart rate, partial atrioventricular block and changes of ST-T segment, accompanied by a decrease in mean coronary flow. No production of hydroxyl radicals was found by HPLC which excluded significant ischemic damage of the myocardium. Good viability of the stained preparation was supported by unchanged electron microscopy. Since in rabbit hearts the VSD-induced arrhythmogenesis was less pronounced, we conclude that the rabbit myocardium is more resistant to the changes triggered by VSD application. It may be due to different properties of the membrane potassium channels in the cardiomyocytes of these two species.

Key words: di-4-ANEPPS — Myocardium — Rabbit — Guinea pig

Introduction

Although the intracellular microelectrode or whole-cell patch clamp techniques still represent the gold standard for recording transmembrane action potentials, the optical method has approached comparable signal-to-noise ratio and thus became a candidate for applications in experimental and clinical studies. Voltage-sensitive dyes (VSDs) provide a powerful new technique for measuring membrane potential in systems where – for reasons of scale, topology, or complexity – the use of electrodes is inconvenient or impossible, e.g. in the presence of external electric fields – uninterrupted and artifact-free recording during pacing stimuli and defibrillation shocks or recording of high-resolution maps, e.g. of cardiac repolarization (Loew 1996).

VSDs have been extensively employed by numerous research groups to record optical action potentials (APs) in a wide variety of heart preparations from single cardiomyocyte to isolated heart. This method represents sophisticated, up-to-date approach to a measurement of fine voltage changes on the membrane of cardiac cell. Simultaneous recordings of transmembrane potential by optical and microelectrode techniques have validated the high fidelity of optical APs as compared with microelectrode recordings and demonstrated that optical APs recorded the classic features of APs from various parts of the conductive system and working myocardium (Bove and Dillon 1998; Choi and Salama 1998, 2000; Dillon et al. 1998; Laurita and Singal 2001).

Correspondence to: Marie Novakova, Department of Physiology, Faculty of Medicine, Masaryk University, Komenského náměstí 2, 662 43 Brno, Czech Republic
E-mail: majka@med.muni.cz

However, this technique faces some limitations. The main one is that the downstroke of the AP is usually disfigured by moving tissue. The classical measurement of AP by means of the microelectrode differs from the optical AP also in such a way that optical recording represents the sum of APs from the cells within the region of tissue and not the AP of a single cell. Also the absolute value of membrane resting potential cannot be obtained unless calibrated with a microelectrode (Choi et al. 1998).

Several groups of VSDs have been introduced (merocyanine, ANEPPS, etc.), out of them those ones from aminonaphthyl-ethenyl-pyridinium (ANEPPS) group are the most consistently used in cardiac preparations (Montana et al. 1989; Loew 1996; Salama 2001). Generally, the VSD has to fulfill several criteria: i) it has to exhibit large fluorescence and/or absorption changes that vary (preferably linearly) with changes of the membrane potential; ii) its optical responses must be specifically related to the changes of membrane potential and not to ion concentration, transmembrane currents, or membrane conductance; iii) the response time of the dye has to lay in microsecond range; iv) the dye should be optically stable in its local environment and not prone to photobleaching upon an exposure to intense light; v) staining of the heart with the dye should not result in pharmacological or toxic effects to the preparation.

The last condition is very important to monitor since the experiments might be of long duration, the whole procedure of loading, washout the dye and the very experiment may take several hours in some experimental set-ups. Thus, it is absolutely necessary to be sure of the viability and quality of the cardiac preparation at the beginning of the AP recording.

The procedure of loading the tissue differs with respect to the experimental model: the cells attached to the coverslips are typically labelled by direct addition of a small amount of dye stock solution to the cell incubation medium. Specific groups of neurons or the isolated heart are loaded by a retrograde perfusion either by a concentrated dye stock solution (neurons) or by diluted dye *via* coronary system (heart). Another possibility is to inject the dye directly to the tissue (e.g. neurons) by microelectrode (microinjection). Usually the preparation is then washed several times to remove excessive dye from the tissue, in case of the isolated heart – from the coronary system (Zochowski et al. 2000; Novakova et al. 2006).

In our experiments in isolated guinea pig and rabbit hearts perfused according to Langendorff, the dye was applied directly into the coronary system. The tissue was loaded by retrograde perfusion of dye stock solution diluted in the perfusion solution. This system is used only in a few laboratories where VSDs are employed for APs measurement (Laurita and Singal 2001; Nygren et al. 2003) and others prefer injection of small volume of VSD stock solution into the bubble trapper of the perfusion set during short period of time. Little is known about the response of cardiac tissue to the procedure of staining and washout from dye, although certain observations indicate that binding of the dye to the cardiac cell membranes changes the overall situation there (Cheng et al. 1998; Nygren et al. 2003).

In our pilot experiments we accidentally noticed certain changes of electrogram of isolated hearts during staining with VSD di-4-ANEPPS. Since our experiments are of long duration we were worried about the quality of preparation. Moreover, in our experimental set-up recording of APs is continuous and thus the tissue is illuminated for a long time. In order to test the viability of tissue in our experimental model, touchless recording of 3D-electrogram together with the measurement of mean coronary flow (CF) was performed. Ever since we have observed typical changes of electrograms and of CF during the staining procedure and these changes persisted up to certain level also during washout period. By means of high-performance liquid chromatography (HPLC) we tested whether the application of di-4-ANEPPS was accompanied by the formation of hydroxyl radicals. Electron microscopy was employed to check the putative ultrastructural changes in the tissue exposed to the dye. Finally, we compared two ways of staining the heart with VSD to get an idea about the persistence of dye in the tissue and to exclude the possibility that long exposure to the dye during the staining leads to the tissue damage.

Materials and Methods

Isolated perfused heart according to Langendorff

The perfusion apparatus for small animal hearts (Figure 1) based on Langendorff technique was modified in our laboratory for pharmacological experiments in which more than one reservoir was needed (Novakova et al. 2000). The common glass bath is used to keep the desired temperature in all reservoirs. Each reservoir is oxygenated separately. A system of four-way stop-cocks allows rapid switching of solutions between respective reservoirs. Small diameter of the connecting tubes accounts for a small dead space. This is very important for minimizing variations in temperature when switching from one solution to another. A special system keeps the perfusion pressure constant and equal in all reservoirs in spite of different amounts of solution.

Briefly, the animal was deeply anaesthetized by ketamin (60 mg/kg of body mass) and xylazin (2 mg/kg of b.m.), artificially ventilated and the chest was opened. Then the heart was excised with a sufficiently long segment of ascending

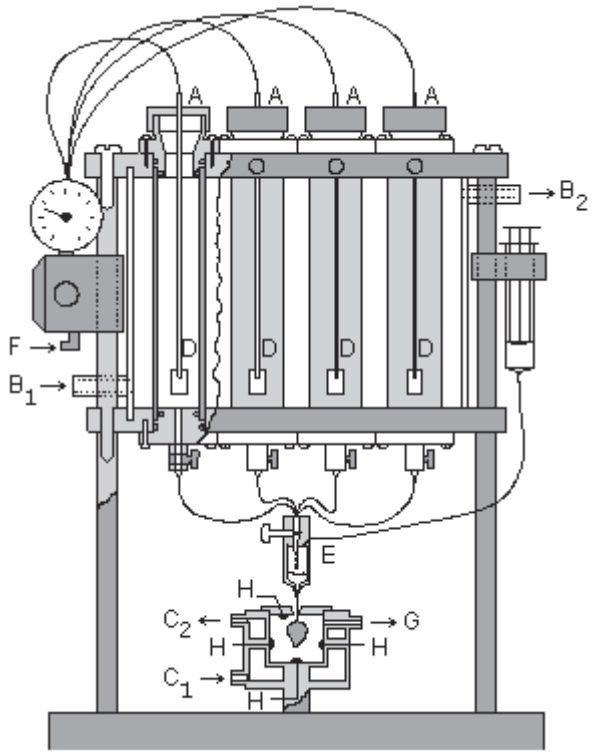

Figure 1. Modified perfusion set according to Langendorff. Four reservoirs (A) filled with perfusion solution are placed in a common bath (connected to a thermostat – B_1, B_2). The heart is placed in a small double-walled bath connected to the thermostat as well (C_1, C_2). The solution in every reservoir is separately oxygenated (D). Heated and oxygenated perfusate is driven to the heart fixed on the cannula at the tip of a bubble-trapper (E). The perfusion pressure is maintained at a preset level by a special control system (F), connected to all reservoirs and to the cylindre with O_2/CO_2 mixture. The perfusate leaving the heart drops into the solution in the bath. The overflow-tube (G) is placed in the wall of the bath close to proximal margin. Six silver-silver chloride disc electrodes are placed on the inner surface of the bath (H).

aorta. The aorta was cannulated, the heart mounted in the Langendorff apparatus and placed in thermostat-controlled bath (37°C) filled with Krebs–Henseleit solution of following composition (in mmol/l): NaCl 118, $NaHCO_3$ 24, KCl 4.2, KH_2PO_4 1.2, $MgCl_2$ 1.2, glucose 5.5, taurine 10 and $CaCl_2$ 1.2. The solution is oxygenated with 95% O_2 and 5% CO_2. The isolated heart is then perfused with the same solution at the constant perfusion pressure (80 mm Hg) for 25–30 min – control period. All hearts exhibiting any dysrhytmias during this period are discarded.

In this study, hearts of 14 guinea pigs of non-specified breed (both sexes, average weight 366 ± 86 g) and 30 New Zealand rabbits (both sexes, average weight 2950 ± 380 g) were included.

Electrogram and mean CF

During the whole experiment, electrogram was recorded and mean CF monitored. The electrogram was recorded by the touch-free method (Uematsu et al. 1987). Six silver-silver chloride disc electrodes (4 mm in diameter) are placed on the inner surface of the bath. Electrogram signals are recorded from three orthogonal bipolar leads (x, y, and z). The signals are amplified and digitized at a sampling rate of 500 Hz by a three-channel, 16-bit analog to digital converter. The maximum amplitude of recorded signals varies between 100 μV and 500 μV, depending on the subject. The mean CF was measured every fifth minute during the whole experiment.

Staining the heart

Each experiment proceeds in four steps: isolation of the heart, control, staining with the dye, and measurement of optical APs under the experimental protocols (ischemia and reperfusion, pharmacological interventions, etc.). The heart is exposed to voltage-sensitive dye di-4-ANEPPS (Molecular Probes, Eugene, OR, USA) diluted in Krebs–Henseleit solution to the concentration of 2 μmol/l (stock solution either in DMSO or DMF, 2 mmol/l). The tissue is perfused with this mixture for approximately 20 min. Again, the electrogram and mean CF are monitored. The dye is washed out for the same period of time as was the staining. Then the heart is ready for optical recording of APs.

In most of laboratories, another way of staining with VSD is used – direct application of small amount of concentrated dye into the bubble trapper by means of microsyringe or pump. Therefore, in final part of our study we compared these two different ways of staining in rabbit hearts – some hearts were stained by regular procedure – e.g. "slow" application of diluted dye into coronary system at speed given by CF and in some heart "fast" staining (application of 20 μl of stock solution in the aortic cannula, 5 min washout and then measurement) was applied.

High performance liquid chromatography

Isolated hearts were perfused with Krebs–Henseleit solution containing 1 mmol/l salicylate during control period and then with Krebs–Henseleit buffer containing 1 mmol/l salicylate and di-4-ANEPPS for loading. Hydroxylated products of salicylic acid were analyzed in the coronary effluents. Determination of 2.5-di-hydroxy benzoic acid (2.5-DHBA) rather than 2.3-DHBA was used because of its greater sensitivity for the quantification of hydroxyl radicals' productions. The effluents were collected at the end of both perfusion periods (with and without di-4-ANEPPS) and stored at –80°C until assayed by HPLC electrochemical de-

tection. Retention times for the peak 2.5-DHBA and salicylic acid were verified by injecting standards.

The HPLC apparatus consisted of high pressure LCP 4000.1 pump, electrochemical detector Coulochem II with analytical cell model 5010 (ESA, Chelmsford, MA, USA) and Rheodyne 7125 syringe loading sample injector (Cotati, CA, USA), sample loop 20 μl. The Chromatography Station for Windows version 1.5 (Data Apex, Prague, Czech Republic) was used for the quantification. All analyses were performed on a reversed-phase column (LiChrospher 100 RP 18.5 μm, 100 × 3 mm I.D, Merck) with precolumn (Separon SGX, 5 μm). Detection of 2.5-DHBA and salicylic acid was performed by isocratic elution with the mobile phase containing 20% (v/v) MeOH in the buffer pH 3.6 (0.03 mol/l citric acid and 0.06 mol/l NaH_2PO_4), flow rate 0.5 ml/min. The mobile phase was filtered through nylon membrane filter (0.2 μm pore size, SolVac, USA). Analytes were detected on a dual electrode analytical cell with the first electrode set to oxidize the 2.5-DHBA at +250 mV and the second electrode set to oxidize salicylic acid at +750 mV. A guard cell (model 5020) was placed between the pump and sampler at a potential of +775 mV to oxidize contaminants in mobile phase.

Part of the hearts included in this study was tested on hydroxyl radical production. There was no difference in other measured parameters between the hearts perfused with salicylate and hearts perfused without it.

Electron microscopy

The viability of preparation was checked by electron microscopy. The tissue was prepared by the following procedure: at the end of experiment (washout period), the heart is perfused with 3% solution of glutaraldehyde for 10 min, removed from Langendorff apparatus and the strips 1 × 1 × 3 mm in size were cut from both atria and ventricles. The samples were immediately fixed in a 400 mmol/l solution of glutaraldehyde in 0.1 mol/l phosphate buffer at pH 7.4. Fixation was carried out in two baths of 40 mmol/l OsO_4 solution in phosphate buffer at pH 7.4.

Dehydration, immersion and embedding in Durcupan ACM followed the standard procedure. Ultra thin sections were made on an LKB Nova ultramicrotome and stained with lead citrate or with uranyl acetate and lead citrate. The sections were viewed and photographed in a Philips Morgagni 268D (FEI, The Netherlands) electron microscope.

Results

Perfusion with VSD di-4-ANEPPS caused specific changes of electrograms in all examined hearts. Moreover, there was a difference between guinea pig and rabbit hearts. Figure 2 shows RR interval changes during staining with VSD in both animal models. Each value represents an average of minimum 12 animals. Results are presented as a mean ± S.E.M. Statistical differences among groups were determined by one-way analysis of variance (ANOVA).

RR intervals respond to VSD application with a delay. This delay is affected by CF that is individually different even if using hearts of the same species, sex, age, and similar weight. This effect of VSD on heart excitability is, however, washable only in rabbit hearts; in guinea pig hearts the decrease in heart rate is sustained. These changes are not statistically significant in rabbit hearts.

Beside the changes in the heart rate, in both models various changes in the shape of electrogram recorded during

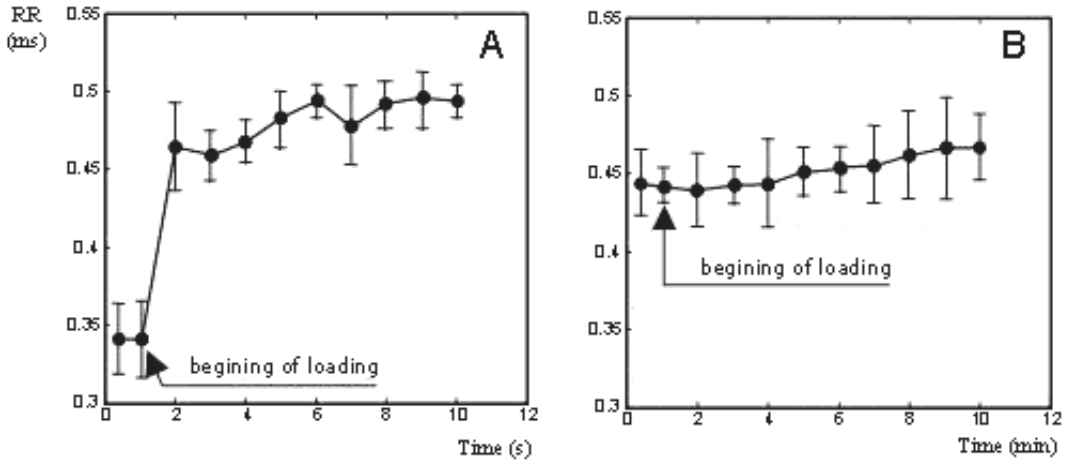

Figure 2. Changes in RR intervals in guinea pig (A) and rabbit (B) heart immediately after dye application (A, time scale in seconds) and during 10-min period of staining (B, time scale in minutes). Note the immediate RR intervals prolongation in guinea pig. This effect is irreversible and significant ($p < 0.05$). RR interval changes in rabbit hearts (B) are subtle and washable (not shown).

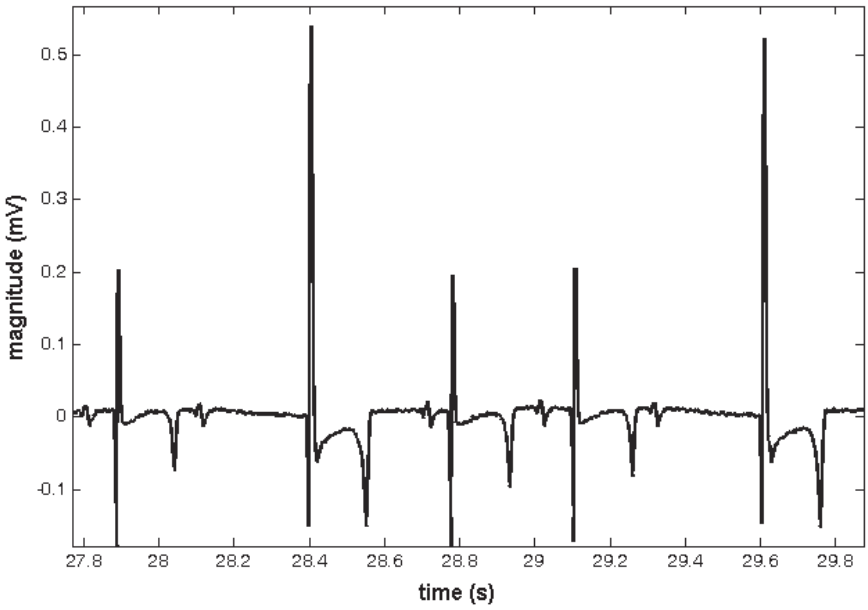

Figure 3. Electrogram of isolated perfused guinea pig heart recorded during perfusion with dye. Note the irregularities of rhythm.

staining were observed – mainly the shape of QRS complex and T wave were often altered by perfusion with the dye. These changes during VSD application were observed in all experiments in guinea pig, and in part of rabbit hearts. Among other changes of electrogram, the most prominent one is "floating" of P wave or partial block in the atrioventricular (AV) node, also more often present in guinea pig hearts. All these changes are partially reversible during the washout period in guinea pig. In rabbit, the changes of electrogram configuration are minor, insignificant and fully washable.

An example of the effect of perfusion with di-4-ANEPPS on electrogram is given in Figure 3 and for the comparison of VSD effect in isolated heart of both species see Figure 4. CF changes are summarized in Figure 5. The mean CF does not significantly change during the period of loading with the dye, however, in the period of washout the decrease of the mean CF can be observed in most of the hearts. Due to inconsistency of the measured data the decrease in CF is insignificant in neither species or situation.

Decrease in the CF might cause ischemic damage of the myocardium and in turn this could explain certain electrophysiological changes observed during staining with VSD and washout of the dye. Thus we decided to test whether hydroxyl radicals were formed during control period and if the presence of di-4-ANEPPS can affect their formation. The method described by Onodera was used (Onodera and Ashraf 1991) that was verified in our previous experiments (Bochorakova et al. 2006). In this method, salicylic acid is added to the perfusion medium and production of hydroxyl radicals is detected on the basis of formation of hydroxylation products of salicylic acid. The 2.5-DHBA can be detected on HPLC. Isolated hearts were perfused in the presence of 1 mmol/l salicylic acid. We analysed the production of 2.5-DHBA in coronary effluents and the effect of di-4-ANEPPS on its formation. We didn't find any peak of 2.5-DHBA in the chromatogram during perfusion period as well as in the presence of di-4-ANEPPS (Figure 6). This implies that the treatment with di-4-ANEPPS during loading period is not followed by the formation of hydroxyl radicals.

Next part of our study was focused on examination of possible ultrastructural changes caused by long-lasting exposure to VSD. In comparison with control hearts, those loaded with di-4-ANEPPS did not reveal any changes detectable by electron microscopy (see Figure 7 for guinea pig myocardium): the tissue was composed of interconnected mono-nucleated cells imbedded in a weave of collagen. The picture contains a large number of myofibrils, striated like in skeletal muscle. A large fraction of the cell volume is occupied by mitochondria. Myofibrils and mitochondria occupy about 85% of the heart cell volume; the rest contains sarcolemma, T-tubules, sarcoplasmic reticulum, intercalated discs, and gap junctions (nexus). Both species were examined and no changes in ultrastructure as a consequence of di-4-ANEPPS binding were observed in either of the examined hearts.

Finally, we decided to compare signal-to-noise ratio (SNR) in rabbit hearts stained with di-4-ANEPPS in both staining procedures. Rabbit was chosen because of its

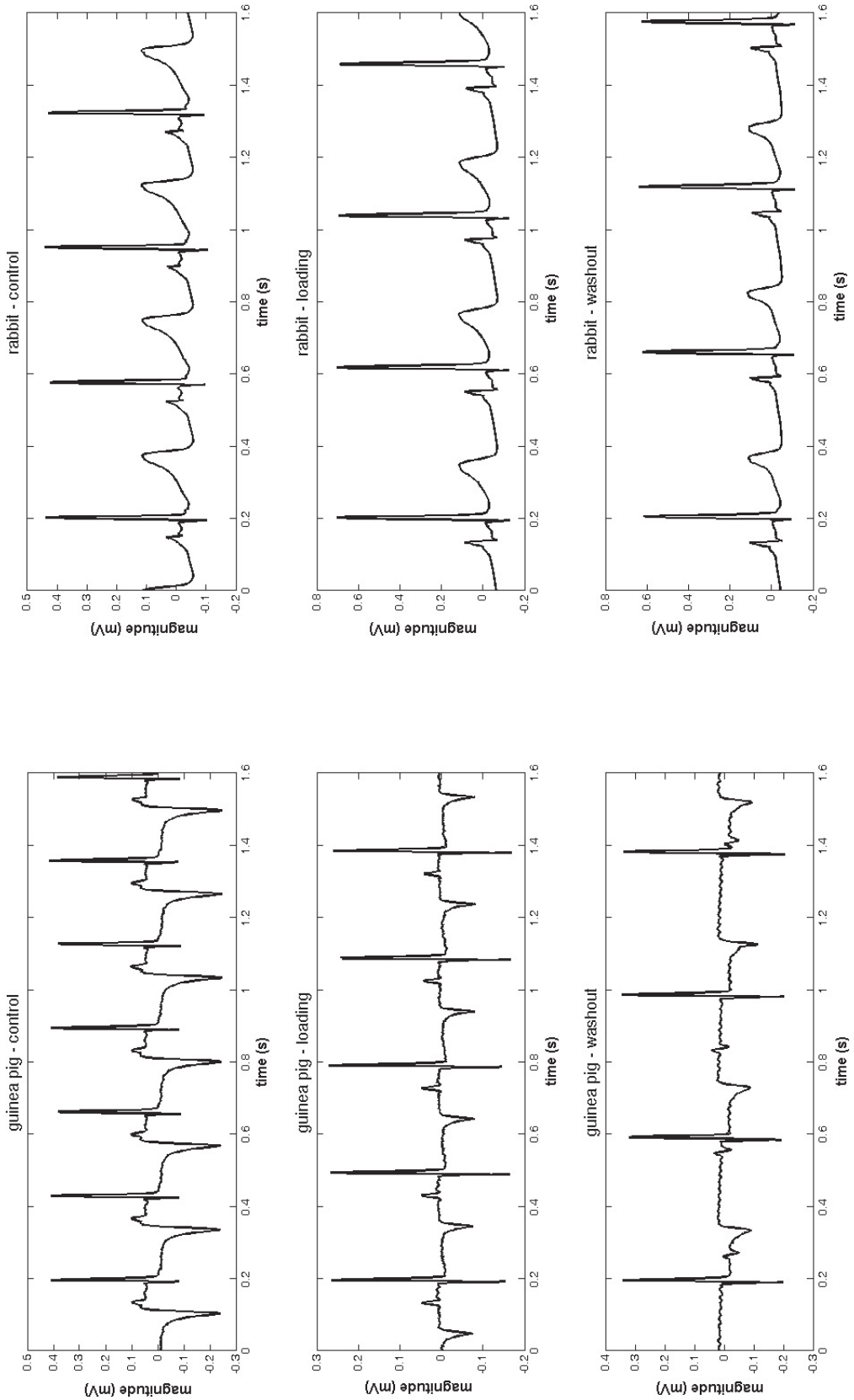

Figure 4. Original records of the effects of VSD on a guinea pig (left panel) and a rabbit (right panel) isolated heart. Note the partial AV block in guinea pig – washout (left bottom).

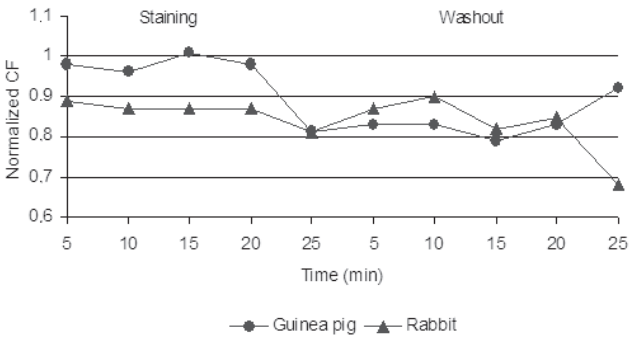

Figure 5. Mean coronary flow (CF) measured during staining and washout period in both animal models. Each value represents an average of minimum 12 animals. Results are presented as a mean (S.E.M. not calculated – the values are normalized to the end of stabilization period). Statistical differences among groups were determined by ANOVA.

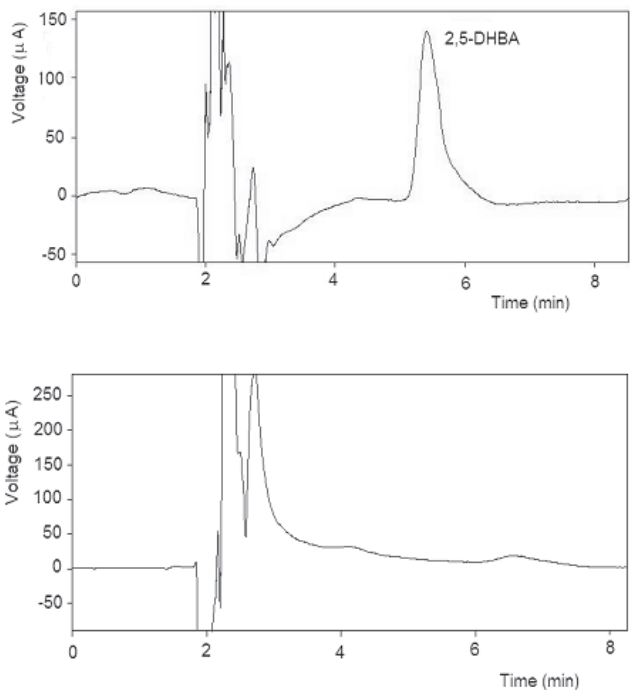

Figure 6. Top: model HPLC chromatogram of the Krebs–Henseleit solution containing standard of 2.5-DHBA. Peak of 2.5-DHBA has retention time 335 s. Bottom: HPLC chromatogram of coronary effluent containing 1 mmol/l salicylate and di-4-ANEPPS. No peak of 2.5-DHBA is seen.

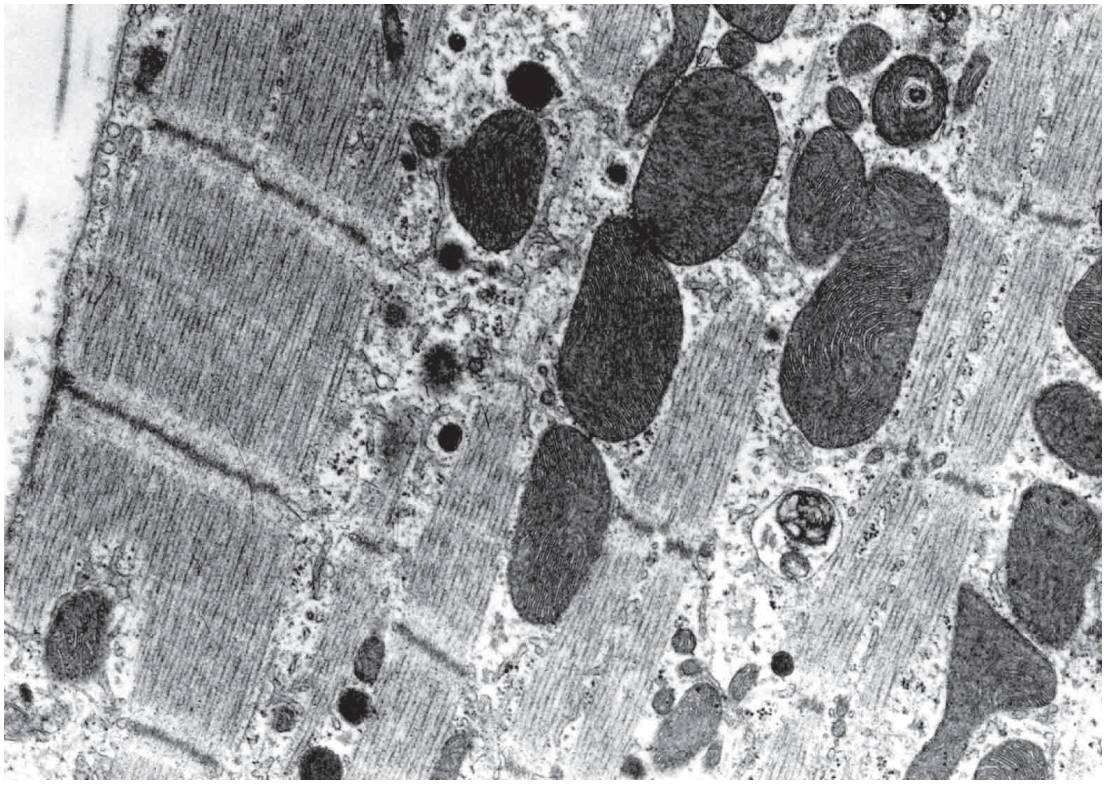

Figure 7. Electronoptic picture of guinea pig heart muscle exposed previously to fixation to VSD di-4-ANEPPS.

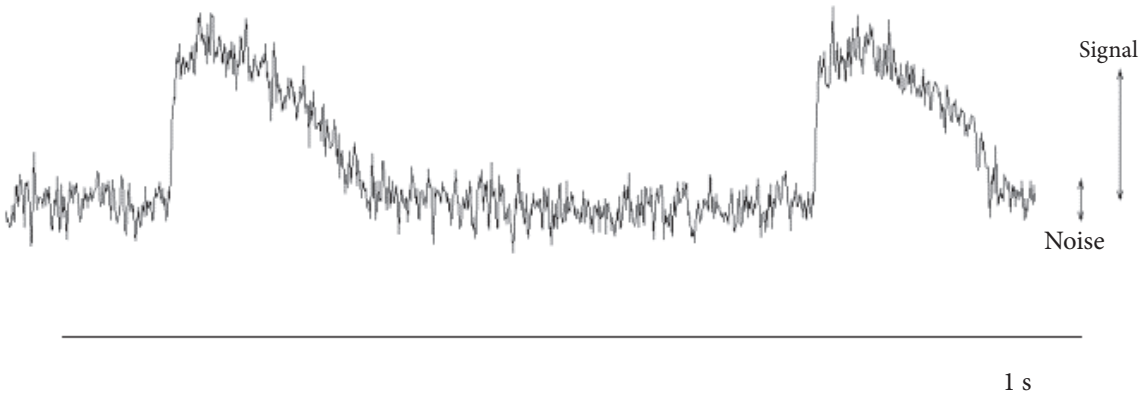

Figure 8. Original recording of APs with marked values of signal and noise. Recording was obtained after approximately 8 min of continuous illumination.

better resistance to changes triggered by VSD application. After the heart was stained and the excess of dye washed out from coronary system, continuous exposure to light source and recording of APs was started. In each minute of recording, AP amplitudes were manually marked in their maximum (Figure 8), SNR was evaluated according to formula

$$SNR = 20 \times \log (signal/noise)$$

and obtained values were plotted in Figure 9.

It is obvious that slower staining with low concentration of dye applied into coronary system together with perfusion solution (Method I in Figure 9) brings tissue with higher SNR and also that the obtained signal is smoother. Persistence of dye in the myocardium in this case is quite high in comparison with myocardium stained with small amount of dye applied in one bolus into the perfusion system. Fading of the signal during continuous illumination of the heart in Method II is quite fast.

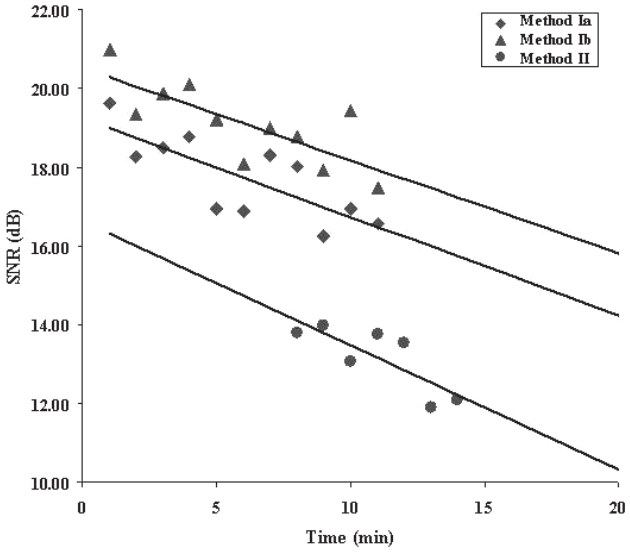

Figure 9. Changes of signal-to-noise ratio (SNR) in rabbit isolated hearts stained with di-4-ANEPPS during continuous illumination. Method I – slow staining (a and b represent two different experiments), Method II – fast staining. Linear trends are marked.

Discussion

The possibility of recording the dynamic changes of the transmembrane potential of excitable cells by optical means was first suggested already in 1968. The first cardiac application was then reported in 1981 – the localization of pacemaker activity in embryonic heart preparation. Since then the method has been improved and numerous VSDs from various chemical groups have been tested (Montana el al. 1989; Salama et al. 2005). Several problems had to be solved before these new dyes were accepted for everyday laboratory practice. One of the most important tasks was to minimize side effects of the dye on the preparation in the absence and presence of light (Salama 2001). Most prominent pharmacological effect of VSDs on cardiac tissue is so-called photodynamic or phototoxic damage. The exact mechanism of these effects remains unknown but undoubtedly it is very complex. Formation of free radicals or direct interaction with the voltage-gated calcium and/or potassium channels have been suggested, which may result in altered conductivity and the time-dependent gating (Cheng et al. 1998; Nygren et al. 2003; Qin et al. 2003).

Our data presented in this study support the idea of direct effect of VSD di-4-ANEPPS on the conductive system and

working myocardium of the guinea pig and rabbit heart similarly as previously reported in rat myocardium by Nygren et al. (2003). Quite typical observation in our experiments was slowing of the heart rate and a partial block in AV node. Accompanying changes of the shape of electrogram curve favor the idea of direct effect of the dye on cardiac ionic channels. Since T wave is often impaired in its shape and amplitude during the staining and washout periods, we assume that predominantly potassium channels are affected.

Most often used experimental models in basic cardiology research – rat, guinea pig and rabbit hearts – differ mainly in repolarization phase of action potential. It is caused by the fact that guinea pig ventricular cardiomyocytes do not develop transient outward current which – in turn – is present in rat and about half of the rabbit ventricular myocytes. Moreover, delayed rectifier current of relatively high amplitude has been found in guinea pig cardiac cells on the contrary to negligible or even absent delayed rectifier current in rat and rabbit. Inward rectifier potassium current is similar in rabbit and guinea pig (Varró et al. 1993). Thus, we can presume that different response of guinea pig and rabbit myocardium to staining with di-4-ANEPPS in our experiments is caused by the effect of this dye on characteristics of delayed rectifier and/or transient outward currents.

Our results concerning electrophysiological changes caused by VSD are in agreement with the above cited study in rat myocardium (Nygren et al. 2003). Namely, AV blocks of various degrees, which are transient and of short duration in rabbit myocardium and more sustained in guinea pig hearts, were observed in rat heart muscle as well. Moreover, various changes of electrogram mainly in repolarization part (ST segment and T wave) accompany staining with di-4-ANEPPS. Again, these changes are more prominent in guinea pig myocardium. Recently, involvement of impaired calcium cycling in direct effect of di-4-ANEPPS on pig hearts (Qin et al. 2003) and positive inotropic effect of another VSD, RH421 in rat myocardium were studied (Cheng et al. 1998). However, when studied in patch clamp experiments, ventricular cardiomyocytes of rat, guinea pig and rabbit did not show any significant differences in calcium inward current (Varró et al. 1993). Nevertheless, the effect of di-4-ANEPPS on conductivity in AV node (present as AV blocks) implies the possibility that slow calcium current in pacemaker cells is affected by the dye.

A decrease in the mean CF observed during staining but mainly during the washout period outlasted in various degrees till the end of the experiment. The explanation of this phenomenon is very difficult since CF is only subsidiary information and it is well known that this parameter depends on many factors. However, we did not find any production of hydroxyl radicals in consequence to staining of the cardiac muscle with voltage-sensitive dye and thus we can exclude the possibility that ischemia – which might be caused by decreased CF – is a reason for observed electrophysiological changes. Also morphological examination did not bring any light into this problem. It seems that application of VSD di-4-ANEPPS causes vasoconstriction in coronary system in isolated guinea pig and partially also rabbit hearts perfused according to Langendorff without any functional or morphological consequences. This data are contradictory to findings of Nygren et al. (2003) who observed transient coronary vasodilatation in rat isolated hearts perfused according to Langendorff after application of di-4-ANEPPS. Yet there are certain differences in their experimental set-up which may explain this incongruity: perfusion pressure was monitored but in our set-up it is kept constant throughout the experiment to ensure proper perfusion during all its phases; the temperature during staining was maintained at 32°C, but in our experiments we worked strictly at physiological temperature of 37°C; and last but not least – rat myocardium differs in many aspects from other species.

Most of laboratories use to stain the myocardium by concentrated dye as a bolus. During short period of staining in this case hardly any electrophysiological changes can be detected. The staining procedure used in our laboratory gives us the opportunity to obtain preparation with quite high persistence of the dye in the stained tissue. We have proved that although certain electrophysiological changes are present in the hearts of both species, at least in rabbit these changes are mostly reversible and thus rabbit myocardium can be stained with di-4-ANEPPS by low concentration of the dye applied into the coronary system and be considered a reliable model for electrophysiolocal studies.

Acknowledgement. All experiments followed the guidelines for animal treatment approved by local authorities and conformed to the EU law. This work was supported by the grant projects of the Grant Agency of the Czech Republic – GACR 102/07/1473, GACR 102/07/P521 and by project MSM 0021622402 of the Ministry of Education of the Czech Republic. The authors wish to thank Prof. Pavel Braveny for fruitful discussion over the manuscript, and Branislava Vyoralova and Drahomira Hradilova for technical help.

References

Bochořáková H., Paulová H., Nováková M., Táborská E. (2006): Determination of hydroxyl radicals in perfused rat hearts by high performance liquid chromatography with coulochemical detection. In: Proceedings of XX. Biochemical Meeting. Page 329

Bove R. T., Dillon S. M. (1998): Optically imaging cardiac activation with a laser system. IEEE Engineering in Medicine and Biology. Pp. 84–94

Cheng Y., Van Wagoner D. R., Mazgalev T. N., Tchou P. J., Efimov I. R. (1998): Voltage-sensitive dye RH421 increases contractility of cardiac muscle. Can. J. Physiol. Pharmacol. **76**, 1146–1150

Choi B. R., Salama G. (1998): Optical mapping of atrioventricular node reveals a conduction barrier between atrial and nodal cells. Am. J. Physiol., Heart Circ. Physiol. **274**, H829–845

Choi B. R., Salama G. (2000): Simultaneous maps of optical action potentials and calcium transients in guinea pig hearts: mechanisms underlying concordant alternans. J. Physiol. **529**, 171–188

Dillon S. M., Kerner T. E., Hoffman J., Menz V., Li K. S., Michele J. J. (1998): A system for *in-vivo* cardiac optical mapping. IEEE Engineering in Medicine and Biology. Pp. 95–108

Laurita R. K., Singal A. (2001): Mapping action potentials and calcium transients simultaneously from the intact heart. Am. J. Physiol., Heart Circ. Physiol. **280,** H2053–2060

Loew L. M. (1996): Potentiometric dyes: Imaging electrical activity of cell membrane. Pure Appl. Chem. **68**, 1405–1409

Montana V., Farkas D. L., Loew L. M. (1989): Dual-wavelength ratiometric fluorescence measurements of membrane potential. Biochemistry **28**, 4536–4539

Novakova M., Blaha M., Bardonova J., Provaznik I. (2006): Comparison of the tissue response during the loading with voltage-sensitive dye in two animal models. Comput. Cardiol. **33**, 577–580

Nováková M., Moudr J., Bravený P. (2000): A modified perfusion system for pharmacological studies in isolated hearts. In: Analysis of Biomedical Signals and Images. 15th Biennial International Eurasip Conference Biosignal. Pp. 162–164, Vutium Press, University of Technology, Brno, Czech Republic

Nygren A., Kondo C., Clark R. B., Giles W. R. (2003): Voltage-sensitive dye mapping in Langendorff-perfused rat hearts. Am. J. Physiol., Heart Circ. Physiol. **284**, H892–902

Onodera T., Ashraf M. (1991): Detection of hydroxyl radicals in the post-ischemic reperfused heart using salicylate as a trapping agent. J. Mol. Cell. Cardiol. **23**, 365–370

Qin H., Kay M. W., Chattipakorn N., Redden D. T., Ideker R. E., Rogers J. M. (2003): Effects of heart isolation, voltage-sensitive dye, and electromechanical uncoupling agents on ventricular fibrillation. Am. J. Physiol., Heart Circ. Physiol. **284,** H1818–1826

Salama G. (2001): Optical mapping: background and historical perspective. In: Optical Mapping of Cardiac Excitation and Arrhythmias (Eds. D. S. Rosenbaum and J. Jalife), Chapter 1, pp. 9–31, Futura Publishing Company, Inc.

Salama G., Choi B. R., Azour G., Lavasani M., Tumbev V., Salzber B. M., Patrik M. J., Ernst L. A., Waggoner A. S. (2005): Properties of new, long-wavelength, voltage-sensitive dyes in the heart. J. Membr. Biol. **208**, 125–140

Uematsu T., Vozeh S., Ha H. R., Follath F., Nakashima M. (1987): Method for stable measurement of the electrocardiogram in isolated guinea pig heart. J. Pharmacol. Methods **18**. 179–185

Varró A., Lathrop D. A., Hester S. B., Nánási P. P., Papp J. G. Y. (1993): Ionic currents and action potentials in rabbit, rat, and guinea pig ventricular myocytes. Basic Res. Cardiol. **88**, 93–102

Zochowski M., Wachowiak M., Falk C. X., Cohen L. B., Lam Y. W., Antic S., Zecevic D. (2000): Imaging membrane potential with voltage-sensitive dyes. Biol. Bull. **198**, 1–21

Final version accepted: January 15, 2008